УДК 550. 834К DOI: https://doi.org/10.24028/gj.v45i6.293306

The correctness of the finite-difference problems of the time- and wave fields continuation for the migration image of the basement boundary

O. Verpakhovska, O. Chorna, 2023

S.I. Subbotin Institute of Geophysics of the National Academy of Sciences of Ukraine, Kyiv, Ukraine
Received 18 July 2023

In modern seismic exploration, the migration procedure plays an important role for further interpretation of the observed data. It is the migration that makes it possible to display the deep structure of the geological section based on the dynamic characteristics of the registered wave fields.

When processing WARRP (wide angle reflection/refraction profiling) seismic data, standard migration methods are ineffective, which is due to the peculiarities of observation systems. All existing migration methods are mainly based on reflected waves, which have a limited registration interval. The wave field on WARRP is observed at distances from sources that reach several hundred kilometers, and the uneven step between receivers is on average 1—3 km. Under such conditions, it is difficult and sometimes impossible to separate the reflected waves.

The finite-difference reflection/refraction migration developed at the Subbotin Institute of Geophysics of the National Academy of Sciences of Ukraine has proven its effectiveness in constructing migration images of the depth structure of the section based on WARRP data observed in various regions of the world. The main difference of this migration method is the use of refracted waves as reference waves registered in the large offsets. At the same time, there is a question of the correctness of the reproduction of the depth structure of the section on the migration image, which depends on the correctness of the calculation methods. The algorithm of finite-difference reflection/refraction migration contains a continuation of the time and wave fields.

The article presents a proof of the mathematical correctness of the solution of the eikonal differential equations and the scalar wave equation by the finite-difference method, on which are based the continuation of the time and wave fields, respectively.

The given comparison of the formed migration images and the velocity models, calculated by the ray-tracing method, of the upper crust along the PANCAKE and TTZ-South profiles allows us to assert that the combination of the results of kinematic and dynamic processing of WARRP data allows to increase the informativeness of their further interpretation.

Key words: correctness, migration of reflected/refracted waves, inverse continuation of the wave field, direct continuation of the time field, WARRP profiles (DSS), eikonal equation, wave equation.

Introduction. Seismic migration is an integral part of seismic data processing. It provides a picture of the internal structure of a complex geological section in the dynamic characteristics of the observed wave field. According to [Gardner, 1985], before migration, seismic data are no more than registered traces of echo signals, waves reflected from

Citation: *Verpakhovska, O., & Chorna, O.* (2023). The correctness of the finite-difference problems of the time- and wave fields continuation for the migration image of the basement boundary. *Geofizicheskiy Zhurnal*, *45*(6), 36—49. https://doi.org/10.24028/gj.v45i6.293306.

Publisher Subbotin Institute of Geophysics of the NAS of Ukraine, 2023. This is an open access article under the CC BY-NC-SA license (https://creativecommons.org/licenses/by-nc-sa/4.0/).

subsurface anomalies. The migration process is aimed at transforming the observed wave field, which is a record of the waves' passage through the geological environment over time, into a depth section of this environment, which is reflected in the dynamic characteristics of the observed wave field. At the same time, migration translates the time scale of seismic section to its depth scale and, through mathematical calculations, helps to relate the geological objects to their correct position in space.

Standard migration techniques are generally based on the processing of reflected waves of CDP data and are applied pre- and post-stacking [Baysal et al., 1983; Claerbout, 1985; Sinha et al., 2009]. When processing seismic data observed by the deep seismic sounding WARRP (wide angle reflection/refraction profiling) — the analogue of DSS [Makris et al., 1999; White, 2020]), standard migration techniques are inefficient because the observing systems for CDP and WARRP are different.

For example, for the WARRP, shots and receivers are placed irregularly along the profile: the average step between the points of explosion is 30—60 km and between the receivers — 0.5—3 km. At the same time, the registration of the wave field is carried out at distances from the shots that reach several hundred kilometers. Meanwhile, CDP-reflection data provide a step between shots of 0.05 km and between receivers — 0.025 km. Therefore, it is at least incorrect to compare the obtained migration sections from the CDP and WARRP data. These images contain complementary information about the deep structure of the research region allowing a more complete interpretation [Verpakhovska et al., 2017].

To find a way to apply seismic migration methods to WARRP data, a finitedifference reflection/refraction migration method was developed at the Institute of S.I. Subbotin Institute of Geophysics of the National Academy of Sciences of Ukraine. This techni-que yields an image of the deep structure of the crust and upper mantle based on wave fields registered several hundred kilometers from the source.

The main differences between this method and the existing finite-difference migration methods such as Reverse Time Migration (RTM) [Zhang et al., 2010; Zhou et al., 2018], consist in the use of refracted waves as a reference and the direct continuation of the time field and inverse continuation of the wave field, in contrast to RTM-type migration procedures that use only direct and inverse continuation of the wave field [Verpakhovskaya, 2021].

Of the existing developments in this direction [Zhang et al., 2010; Sun et al., 2012], the finite-difference migration of the field of reflected and refracted waves is the only one approbated in different areas of the world where regional WARRP surveys were performed [Pilipenko et al., 2011; Verpakhovskaya et al., 2015, 2018, 2021; Yegorova et al., 2022; Murovskaya et al., 2023].

At the same time, there arises the question of reproducibility of the deep structure image based on the migration section. In particular, it depends on the correctness of the calculation methods. The article presents proofs of the mathematical correctness of the eikonal differential equation solution and the scalar wave equation solution, which are the basis for the continuations of time- and wave fields when using the finite-difference method.

As a practical example of applying the finite-difference reflection/refraction migration, we provide generated images of the foundation boundary along the PANCAKE and TTZ-South seismic profiles.

Along these profiles, the S.I. Subbotin Institute of Geophysics of the National Academy of Sciences of Ukraine, together with foreign colleagues, carried out seismic observations by the WARRP method within international projects [Starostenko et al., 2013; Janik et al., 2021]. These two profiles are located in the transition area of the Western European platform to the Eastern European platform. At the same time, they are perpendicular to each other, which is of particular interest for the study of the deep structure of this region. The wave fields registered along the profiles were processed by the ray-tracing method; as a result, velocity models were obtained. This

result was obtained only on the basis of the kinematic characteristics of the observed wave field. Including the field's dynamic characteristics using the finite-difference reflection/refraction migration will provide an opportunity to obtain additional details of the deep structure of the area.

Method and theory. The wave field registered by the WARRP method has a complex nature. It contains different types of waves, among which it is possible to reliably distinguish and track refracted waves from the distribution boundaries contrasting in velocity, such as the crystalline basement. Including selected refracted waves registered at large offsets is the main idea of the finite-difference reflection/refraction migration method. The theoretical basis of this method differs from the standard reflection migration since the refracted waves pass through two layers at significantly different velocities (Fig. 1): $V_2(x,z) >> V_1(x,z)$ [Verpakhovskaya et al., 2018]. The finite-difference reflection/refraction migration is based on the principle of the pre-stack migration; therefore, it is performed for each shot point gather separately.

The main elements of the algorithm are transfer of the source (*shot*) to the refraction boundary (point *O*); direct continuation of the time field $T(x, z)$ taking into account the velocity of wave propagation in the refracting layer; inverse continuation of the wave field $U(x, z, t)$ from the surface to depth with a velocity model characteristic of the covering layer.

According to the sampling of the values of the continued wave field at the time values that correspond to the times of exit of the refracted wave from the refracting layer, a wave image of the investigated boundary $I(z, x)$ and the layer adjacent to it is formed (in Fig. 1, it is shown by an ellipse) [Verpakhovskaya et al., 2018].

Since the refracted wave passes through two layers with different velocity characteristics, in order to perform dynamic migration of the field of refracted waves, it is necessary

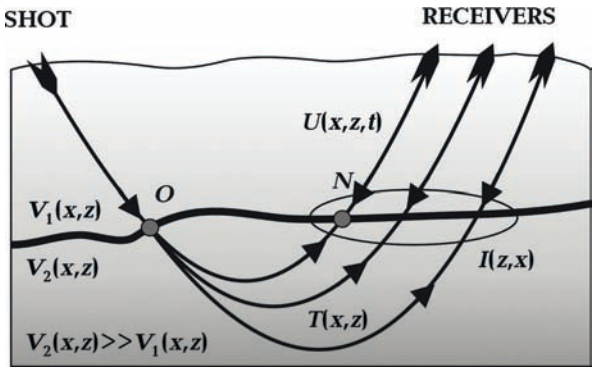

Fig. 1. Algorithm for the finite-difference reflection/refraction migration method.

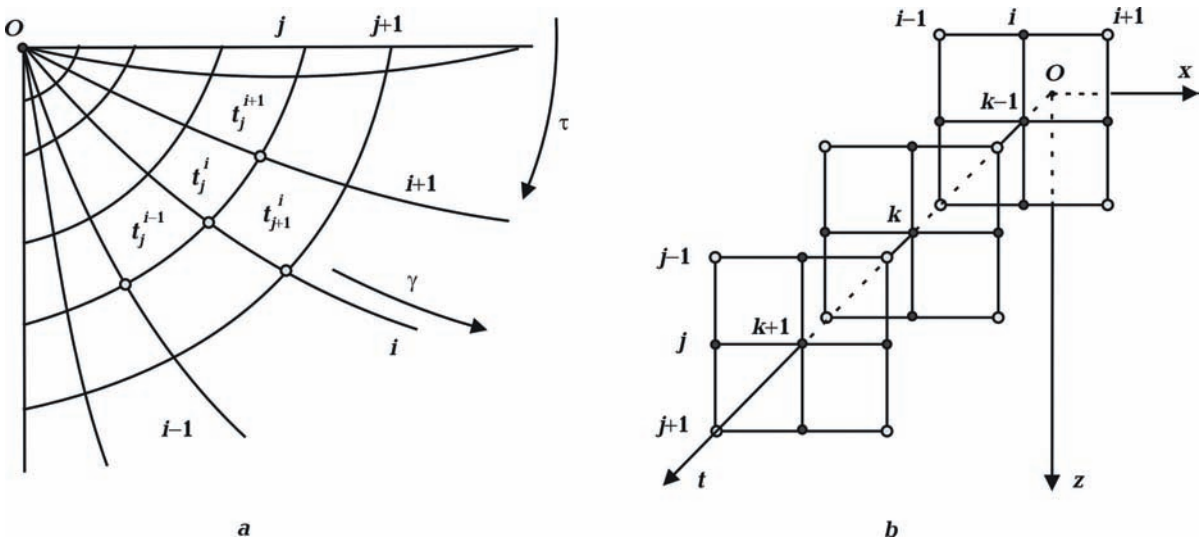

Fig. 2. Finite-difference grid and four-point pattern for the direct continuation of the time field (*a*). A finite-difference three-dimensional spatiotemporal grid pattern for the inverse continuation of the wave field (*b*).

to have separate velocity models for the covering layer and the refracting layer. There must also be information about the depth of occurrence of the refraction boundary in the disturbance point area for its correct transfer.

The numerical implementation of the main elements of the computational process during the finite-difference reflection/refraction migration, namely, the direct continuation of the time field and the inverse continuation of the wave field, is carried out by the finite-difference method for solving differential equations: wave and eikonal. The need to calculate time- and wave fields in an area remote from the source determines the computational process. At the same time, a grid of rays and isochrons is used to continue the time field, and a three-dimensional space-time grid is used to continue the wave field (Fig. 2). The choice of grids guarantees the correctness of the velocity-contrasting boundary of the distribution of a geological section with the involvement of refracted waves.

We shall consider the algorithm for the two-dimensional version in more detail. We shall also evaluate the correctness of mathematical calculations for direct continuation of the time field and inverse continuation of the wave field by the finite-difference method.

By a conditional movement of the disturbance source from the day surface to point *O* (see Fig. 1) located on the refracting boundary and the corresponding to the waves' point of entry into the refracting layer, the problem of ambiguity in the formation of images from the kinematics of refracted waves is solved. Such shot displacement is carried out by recalculating the time of passage of the wave of the covering layer. It allows taking into account the sharp change in velocity that occurs at the boundary of the foundation. Before the transfer, the ray of the refracted wave crosses the refracting environment at two points: *O* (*entry point*) and *N* (*exit point*), and after the transfer, only at point *N* (see Fig. 1).

Thus, the problem of forming the refracting boundary image becomes unambiguous and is solved at the moment of the wave's exit from the refracting medium; it allows to reproduce all details of the refracting layer. Such formulation of the problem of forming a migration image of the environment by the field of refracted waves guarantees the unambiguity of its solution. Transferring the shot from the profile line to the boundary of the foundation is done by calculating and replacing the wave arrival time.

To implement the direct continuation of the time field $T(x, z)$, the eikonal equation is solved

$$\frac{1}{V^2(\gamma,\tau)\beta^2\left(\operatorname{ch}\tau-\cos\gamma\cdot\operatorname{sh}\tau\right)^2}+\left[\frac{\partial t(\gamma,\tau)}{\partial\tau}\right]^2+$$
$$+\frac{1}{\operatorname{sh}^2\tau}\left[\frac{\partial t(\gamma,\tau)}{\partial\tau}\right]^2=0, \qquad (1)$$

where $V=V_0(1+\beta z)$ — linear change of velocity with depth z; V_0 — velocity on the daytime surface; β=const, which corresponds to the velocity gradient with depth. Moreover, the velocity function appears directly in the calculation process in a matrix form and so allows forming a dynamic image of the environment of any degree of complexity.

Adjustment of calculation results is ensured by using a special type of difference grids. To solve the problem of the continuation of the time field [Pilipenko et al., 2011], one needs to choose a curvilinear grid of mutually orthogonal isochrons τ and rays γ coming from a point source *O* with a linear change of velocity *V* with depth *z*. In this case, the radial lines of the grid correspond to the real trajectories of the rays of the natural propagation of waves in the remote zone of the source. The connection of isochrones τ and rays γ with the Cartesian coordinate system is determined by the following ratios:

$$\gamma=\operatorname{arctg}\frac{2x}{\beta\left(x^2+z^2\right)+2z},$$

$$\tau=\operatorname{arch}\left[\frac{\beta^2\left(x^2+z^2\right)}{2(\beta z+1)}+1\right]. \qquad (2)$$

The time field is continued sequentially on the lines of isochrones τ=const in the direction of the growth of the coordinate τ according to an explicit difference scheme

[Verpakhovskaya, 2021], the disadvantage of which is its conditional stability [Samarskiy, Gulin, 1973]. The choice of rays arriving at grid nodes with coordinates (i, j+1) within the framework of the grid template (Fig. 2, *a*) [Pilipenko, Verpakhovskaya, 2003] makes it possible to achieve the correctness of the proposed solution.

To implement the finite-difference method of solving the eikonal equation in the closed region of the formation of the environment image, we denote by $\Delta\tau$, $\Delta\gamma$ the steps along the axes of a uniform grid, where the coordinates of the grid along the τ and γ axes correspond to i and j; by t_j^i — the time at the grid node with coordinates i and j. In the proposed notation, the continuation of the time field t_{j+1}^i is calculated according to an explicit difference scheme at each point in space as follows:

$$t_{j+1}^i = t_j^i + \Delta\tau\sqrt{\frac{1}{V^2\beta^2\theta^2} - \frac{1}{sh^2\tau}\left(\frac{t_j^{i+1} - t_j^{i-1}}{2\Delta\gamma}\right)^2} + \frac{\Delta\tau^2}{2}\left(\sqrt{\frac{1}{V^2\beta^2\theta^2} - \frac{1}{sh^2\tau}\left(\frac{t_j^{i+1} - t_j^{i}}{2\Delta\gamma}\right)^2}\right)^{-1} \times \left\{\frac{-\frac{\partial V}{\partial\tau}}{\beta^2V^3\theta^2} - \frac{sh\tau - \cos i_0 ch\tau}{\beta^2V^2\theta^3} + \frac{ch\tau\left(t_j^{i+1} - t_j^{i-1}\right)^2}{4\Delta\gamma^2 sh^3\tau} + \right.$$

$$+ \frac{1}{2\Delta\gamma\, sh^2\tau\sqrt{\frac{1}{V^2\beta^2\theta^2} - \frac{1}{sh^2\tau}\left(\frac{t_j^{i+1} - t_j^{i-1}}{2\Delta\gamma}\right)^2}} \times \left(\frac{-\frac{\partial V}{\partial\gamma}}{\beta^2V^3\theta^2} - \frac{sh\tau\sin\gamma}{\beta^2V^2\theta^3} - \right.$$

$$\left.\left. - \frac{\left(t_j^{i+1} - t_j^{i-1}\right)\left(t_j^{i+1} - 2t_j^i + t_j^{i-1}\right)}{2\Delta\gamma^3 sh^2\tau}\right)\right\}, \qquad (3)$$

where $\theta = ch\tau - \cos\gamma sh\tau$.

At large distances from the disturbance point and sharp differentiation of the velocity in the environment, there is a possibility of a break in the time field. In this case, the time calculation using the difference equation (3) may be incorrect.

In the actual propagation of the wave field, the wave front is smoothed due to nonradiative effects and diffraction, which are not taken into account by the eikonal equation since it describes the behavior of the time field at an infinite frequency of oscillations. However, this problem was solved by omitting such nodes on a separate grid line in which the solution of the eikonal equation (3) is incorrect.

When re-stepping, the time at the missed nodes is calculated according to the scheme of interpolation or extrapolation of the time values at the grid nodes where the difference calculation was successful. Thus, time field defects are smoothed out just as during real wave propagation. It should be noted that such smoothing is used only in the event of an extreme situation. The validity of such an improvement of the finite-difference continuation of the time field was confirmed for complex velocity models of the environment by comparing the obtained results with the time field determined by the direct continuation of the wave field with automatic correlation of the first arrivals of the direct wave to obtain the time at the grid nodes. For the first time, such an improvement in the continuation of the time field was described in the article [Pilipenko et al., 2003].

The inverse continuation of the wave field $U(x, z, t)$ from the surface to the depth is the most complex and resource-intensive computing stage of the migration process.

Scalar differential wave equation of hyperbolic type

$$\frac{\partial^2U(x,z,t)}{\partial x^2} + \frac{\partial^2U(x,z,t)}{\partial z^2} - \frac{1}{V^2}\frac{\partial^2U(x,z,t)}{\partial t^2} = 0, \qquad (4)$$

for $U(x, z, t)$ — which is a function of the wave field corresponding to the distribution of amplitudes of oscillations in a two-dimensional medium by substituting variables

$$x' = x;\ \ z' = z;\ \ t' = t - \frac{x}{V^*},$$

where V^* is the velocity of reduction of the wave field, x is the distance to the source of

oscillation excitation, z is the depth, t is time, comes down to:

$$\frac{\partial^2 U(x,z,t)}{\partial x'^2}+\frac{\partial^2 U(x,z,t)}{\partial z'^2}- \quad (5)$$
$$-\frac{2}{V^*}\frac{\partial^2 U(x,z,t)}{\partial x'\partial t'}-\left(\frac{1}{V^2}-\frac{1}{V^{*2}}\right)\frac{\partial^2 U(x,z,t)}{\partial t'^2}=0.$$

Let us rewrite the equation in a form more convenient for the quadratic finite-difference approximation of the differential equation

$$\frac{\partial^2 u}{\partial t'^2}+\frac{2V^*V^2(x',z')}{V^{*2}-V^2(x',z')}\frac{\partial^2 u}{\partial x'\partial t'}-$$
$$-\frac{V^{*2}V^2(x',z')}{V^{*2}-V^2(x',z')}\left(\frac{\partial^2 u}{\partial x'^2}+\frac{\partial^2 u}{\partial z'^2}\right)=0. \quad (6)$$

The initial problem for the differential equation in partial derivatives is replaced by a finite number of algebraic (difference) equations by finite-difference approximation using a three-dimensional space-time grid template in a limited grid area (Fig. 2, *b*) [Pilipenko, Verpakhovskaya, 2003]:

$$\left(E-\frac{a\Delta t}{2}L_{\dot{x}}-\mu\Delta t^2\left(L_{\bar{x}x}+L_{\bar{z}z}\right)\right)u_{i,j}^{k-1}-$$
$$-\left(2E-\left(2\mu-c\right)\Delta t^2\left(L_{\bar{x}x}+L_{\bar{z}z}\right)\right)u_{i,j}^{k}+$$
$$+\left(E+\frac{a\Delta t}{2}L_{\dot{x}}-\mu\Delta t^2\left(L_{\bar{x}x}+L_{\bar{z}z}\right)\right)u_{i,j}^{k+1}=0, \quad (7)$$

where E is the unary operator; $i=\overline{1,n}$; $j=\overline{1,m}$ — grid coordinates along the x and z coordinate axes respectively, $k=\overline{1,p}$ — grid coordinates along the time axis t; Δx, Δz, Δt — grid steps;

$$a=\frac{2V^*V^2(x,z)}{V^{*2}-V^2(x,z)},\ c=\frac{V^2(x,z)V^{*2}}{V^{*2}-V^2(x,z)},$$
$$L_{\dot{x}}u_{i+1,j}^{k}=\frac{u_{i+1,j}^{k}-u_{i-1,j}^{k}}{2\Delta x},$$
$$L_{\bar{x}x}u_{i,j}^{k}=\frac{u_{i+1,j}^{k}-2u_{i,j}^{k}+u_{i-1,j}^{k}}{\Delta x^2},$$
$$L_{\bar{z}z}u_{i,j}^{k}=\frac{u_{i,j+1}^{k}-2u_{i,j}^{k}+u_{i,j-1}^{k}}{\Delta z^2}.$$

The continuation of the wave field is carried out in a limited grid area, and the maximum coordinates for variable grid coordinates i, j, and k are determined by the boundaries of the area where the image of the refracting layer is supposed to be formed.

The stability of the finite-difference calculation is ensured by μ=const

$$\mu=\frac{1}{4}\cdot\frac{V_r^2V^2(x,z)}{V_r^2-V^2(x,z)}.$$

The obtained difference equation is implicit in the calculation of the value of the wave field in a separate grid node. Since the value of the field $u_{i,j}^{k-1}$ sought at the inverse continuation is simultaneously under the action of differential operators on two axes, x and z, the direct difference solution of equation (7) is rather complicated. To simplify the solution, factorization of the equation (7) is carried out after [Samarskiy, 1983], which consists of splitting the operator at the field value $u_{i,j}^{k-1}$ into a product of two operators along the two coordinate axes x and z accordingly:

$$\left(E-\mu\Delta t^2L_{\bar{z}z}\right)\left(E-\frac{a\Delta t}{2}L_{\dot{x}}-\mu\Delta t^2L_{\bar{x}x}\right)u_{i,j}^{k-1}-$$
$$-\left(2E-\left(2\mu-c\right)\Delta t^2\left(L_{\bar{x}x}+L_{\bar{z}z}\right)\right)u_{i,j}^{k}+$$
$$+\left(E+\frac{a\Delta t}{2}L_{\dot{x}}-\mu\Delta t^2\left(L_{\bar{x}x}+L_{\bar{z}z}\right)-\frac{\mu a\Delta t^3}{2}L_{\bar{z}z}L_{\dot{x}}-\right.$$
$$\left.-\mu^2\Delta t^4L_{\bar{x}x}L_{\bar{z}z}\right)u_{i,j}^{k+1}=0. \quad (8)$$

Difference operators

$$\frac{\mu a\Delta t^3}{2}L_{\bar{z}z}L_{\dot{x}}u_{i,j}^{k+1},\ \mu\Delta t^4L_{\bar{x}x}L_{\bar{z}z}u_{i,j}^{k+1},$$

are necessary to compensate for the difference operators that arose during the splitting of the operators at the value of the field $u_{i,j}^{k-1}$.

The system of equations (9) implements the finite-difference approximation of equation (8):

$$\left(E-\frac{a\Delta t}{2}L_{\dot{x}}-\mu\Delta t^2L_{\bar{x}x}\right)Y_{i,j}=$$
$$=\left(2E-\left(2\mu-c\right)\Delta t^2\left(L_{\bar{x}x}+L_{\bar{z}z}\right)\right)u_{i,j}^{k}-$$
$$-\left(E+\frac{a\Delta t}{2}L_{\dot{x}}-\mu\Delta t^2\left(L_{\bar{x}x}+L_{\bar{z}z}\right)-\right.$$

$$-\frac{\mu a\Delta t^3}{2}L_{\bar{z}z}L_{\dot{x}}-\mu^2\Delta t^4L_{\bar{x}x}L_{\bar{z}z}\Bigg)u_{i,j}^{k+1}, \quad (9)$$

$$\left(E-\frac{\mu\Delta t^2}{\Delta z^2}L_{\bar{z}z}\right)u_{i,j}^{k-1}=Y_{i,j},$$

where $Y_{i,j}$ is an intermediate grid function.

To formulate the finite-difference problem of the inverse continuation of the wave field, the initial (10) and boundary (11) conditions are introduced:

$$u\left(x,z,t_{\max}\right)=0,\ \left.\frac{\partial u\left(x,z,t\right)}{\partial t}\right|_{t=t\max}=0, \quad (10)$$

$$u\left(x,0,t\right)=\overline{u}\left(x,t\right),\ u\left(x_1,z,t\right)=0,$$

$$u\left(x_2,z,t\right)=0,\ u\left(x,z_{\max},0\right)=0. \quad (11)$$

The system of equations (9), together with the initial (10) and boundary (11) conditions, make up the mixed problem of the inverse continuation of the wave field in the parallelepiped ($x_1<x<x_2$, $0<z<z_{\max}$, $0\le t<t_{\max}$).

The scheme (9, 10, 11) assumes that the system of equations (9) is solved at each time step (k–1) of the obliquely angular (oblique-angled) spatio-temporal grid by the sweep method — along the axis x and the axis z on the grid templates (see Fig. 2). The sweep method consists of two parts: 1) «sweep coefficients» are calculated sequentially (direct sweep); 2) a recurring calculation of the unknowns is carried out, starting with u_N, u_{N-1} and ending with u_1, u_0 (inverse sweep) [Godunov, Ryabenkiy, 1977]. Thus, the tridiagonal matrix is solved. Consider the stability of calculations based on the difference equation (8). To do this, we will bring it to the canonical form [Samarskiy, 1983]:

$$B\left(-u_{\dot{t}}\right)+\Delta t^2Ru_{\bar{t}t}+Au=0$$

where in our case:

$$u_{\dot{t}}=\frac{u_{i,j}^{k+1}-u_{i,j}^{k-1}}{2\Delta t},$$

$$u_{\bar{t}t}=\frac{u_{i,j}^{k+1}-2u_{i,j}^{k}+u_{i,j}^{k-1}}{\Delta t^2},$$

$$A=-c\left(L_{\bar{x}x}+L_{\bar{z}z}\right),$$

$$R=\frac{1}{\Delta t^2}E-\mu\left(L_{\bar{x}x}+L_{\bar{z}z}\right),$$

$$B=-aL_{\dot{x}}+\mu a\Delta t^2L_{\dot{x}}L_{\bar{z}z}+2\mu^2\Delta t^3L_{\bar{x}x}L_{\bar{z}z}.$$

The minus before the operator u_t is due to the inverse continuation of the wave field.

To estimate the stability, we will use the theorem [Samarskiy, 1983]:

If the operators A and R are constant, positive, and self-adjoint, then the conditions $B\ge0$ and $R>1/4A$ are sufficient for the stability of the difference scheme (9, 10, 11) according to the initial data.

In the general theory of stability, it is proved that for such linear problems, such as the problem of solving the wave equation, schemes that are stable according to the initial data are stable in general [Samarskiy, Popov, 1980].

Let us check the theorem.

In the difference expression (8) the operator L_x is skew-symmetric, and $L_{\bar{x}x}$ and $L_{\bar{z}z}$ are positive and self-adjoint [Samarskiy, 1983]. Since the region of the continuation of the field is a rectangle, the operators $L_{\bar{x}x}$ and $L_{\bar{z}z}$, and $L_{\dot{x}}$ and $L_{\bar{z}z}$ are commutative, and therefore the operator $L_{\dot{x}}L_{\bar{z}z}$ is skew-symmetric [Samarskiy, Gulin, 1973]. Let us check the positiveness of the operator B. For this, it is necessary to estimate the scalar product (By, y) for all y, belonging to the Hilbert space, excluding y=0,

$$\left(By,y\right)=-a\left(L_{\dot{x}}y,y\right)+\mu a\Delta t\left(L_{\dot{x}}L_{\bar{z}z}y,y\right)+$$
$$+2\mu^2\Delta t^3\left(\left(-L_{\bar{x}x}\right)\left(L_{\bar{z}z}\right)y,y\right).$$

Since $L_{\dot{x}}$ and $L_{\dot{x}}L_{\bar{z}z}$ are skew-symmetric:

$$\left(L_{\dot{x}}L_{\bar{z}z}y,y\right)=0,\ \left(L_{\dot{x}}y,y\right)=0.$$

Thus, $\left(By,y\right)=2\mu^2\Delta t^3\left(\left(-L_{\bar{x}x}\right)\left(L_{\bar{z}z}\right)y,y\right)$.

Such evaluations exist for operators $-L_{\bar{x}x}$ and $L_{\bar{z}z}$ [Samarskiy, Gulin, 1973]:

$$\left(-L_{\bar{x}x}y,y\right)\ge\frac{8\left\|y\right\|^2}{l^2},\ \left(L_{\bar{z}z}y,y\right)\ge\frac{8\left\|y\right\|^2}{r^2}, \quad (12)$$

where l is the grid size by coordinate x, r is the grid size by coordinate z.

Operator inequalities can be treated like ordinary numerical inequalities, provided they consist of commutative and conjugate difference operators [Samarskiy, Gulin, 1973]:

$$2\mu^2\Delta t^3\left(\left(-L_{\bar{x}x}\right)\left(L_{\bar{z}z}\right)y,y\right)\geq$$
$$\geq 2\mu^2\Delta t^3\left(\frac{8\|y\|^2}{l^2}\right)\left(\frac{8\|y\|^2}{r^2}\right).$$

So, it is proved that $B>0$.

The differential expression A is self-adjoint and positive because the operators $-L_{\bar{x}x}$ and $-L_{\bar{z}z}$ are self-adjoint and positive, and c is a positive coefficient. The expression R is also self-adjoint because it consists of self-adjoint operators. It is only necessary to make sure that the inequality is correct:

$$R-\frac{1}{4}A>0, \qquad (13)$$

from which we automatically obtain that $R>0$.

Consider the conditions under which the expression $R-1/4A$ will be greater than zero.

$$R-\frac{1}{4}A=\frac{1}{\Delta t^2}E-\left(\mu\left(L_{\bar{x}x}+L_{\bar{z}z}\right)+\right.$$
$$\left.+\frac{c}{4}\left(L_{\bar{x}x}+L_{\bar{z}z}\right)\right)>\left(\mu-\frac{1}{4}c\right)\left(-L_{\bar{x}x}-L_{\bar{z}z}\right).$$

From this we obtain the estimate:

$$R-\frac{1}{4}A>\left(\mu-\frac{1}{4}c\right)\left(-L_{\bar{x}x}-L_{\bar{z}z}\right).$$

According to (12), the operators $-L_{\bar{x}x}$ and $-L_{\bar{z}z}$ are positive, so condition (13) will be fulfilled if the inequality is satisfied:

$$\left(\mu-\frac{1}{4}c\right)>0. \qquad (14)$$

This inequality is a condition for the stability of calculations according to scheme (9, 10, 11). The parameter μ must be chosen according to the fulfillment of this inequality for the entire region of the continuation of the wave field.

The stability estimate (14) is obtained under the condition of constancy of the coefficients in the difference equation. In general, the coefficients can be variable. According to the principle of frozen coefficients [Samarskiy, 1983], the stability condition must be fulfilled at the maximum value of the coefficient c.

Therefore, to successfully use the improved finite-difference scheme, it is necessary to ensure its correctness. It requires satisfactory approximation of the differential equation by the finite difference one and stability of a finite-difference calculation.

The first condition is fulfilled due to the introduction of additional terms in equation (7), which compensate for the decrease in the degree of approximation due to the factorization procedure. Thus, the desired quadratic degree of approximation of the differential equation (6) by the finite difference one (7) is preserved.

A study of the stability of the finite-difference calculation was performed by the proposed difference scheme (9, 10, 11). It determined condition (14) under which the calculations are stable. The finite-difference equation (6) does not impose any restrictions on the behavior of the velocity function $V_{i,j}$. However, the calculation according to the system (6) requires significant computing resources. By tests on model and real seismic materials, the continuation of the wave field according to the scheme (9, 10, 11) is carried out correctly even with a very complex velocity distribution in the environment.

Imaging the velocity-contrasting boundary of the geological environment along the profile using the finite-difference reflection/refraction migration method is done by summing individual migration images obtained for each shot point gather. At the same time, to correctly represent the boundary's structural and the adjacent refractive layer, it is necessary to carefully analyze and compare the obtained migration images for each shot point gather and gradually reconstruct the general depth image of the geological structure along the profile.

At the same time, in order to form an image of each disturbance, it is important to have its migration image from different sources located on both sides of the disturbance since, in order to image its true form, it is necessary to sum up the parts of the image of the selected boundary interval from different sides.

This is because the principle of forming an image of the medium in the region where refracted waves exit into the top layer, used in finite-difference reflection/refraction migration, presupposes looking at the boundary at

the angle of refraction from the source side.

Therefore, to obtain the actual form of the disturbance, it is necessary to compare the opposite migration images. This approach was successfully tested on several model examples and real seismic observations. In the article, the application of this approach is demonstrated by an example of the formation of an image of the upper-crust structure based on the data of the PANCAKE and TTZ-South regional profiles.

Practical example. The seismic regional profiles of PANCAKE and TTZ-South were carried out by the WARRP method in the area of the transition of the Western European Platform to the Eastern European Platform [Starostenko et al., 2013; Janik et al., 2021]. These two profiles are of interest because they run perpendicular to each other and the application of finite-difference reflection/refraction migration to them made it possible to obtain additional information about the structure of the boundary and the thickness of the foundation in this area.

The PANCAKE (PANnonian-Carpathians-Cratonic Europe) regional profile (Fig. 3), extending from the East European Craton to the Pannonian Basin, is 645 km long, of which 157 km pass through Hungary and 488 km through Ukraine [Starostenko et al., 2013].

This WARRP profile was carried out in 2008 by Ukrainian researchers of the S.I. Subbotin Institute of Geophysics of the National Academy of Sciences of Ukraine together with the

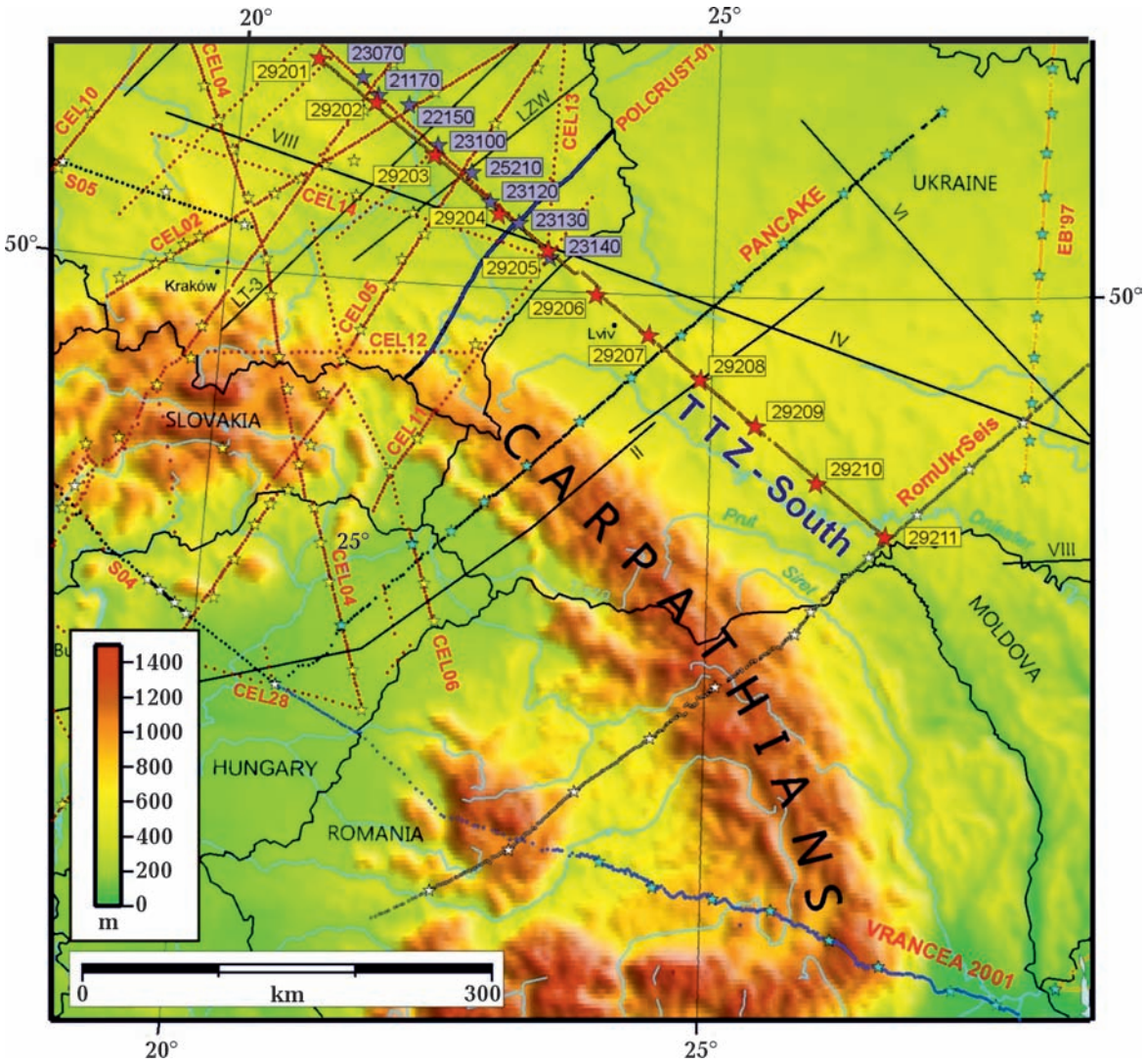

Fig. 3. Regional profiles of PANCAKE and TTZ-South.

State Geophysical Enterprise «Ukrgeofizika» with the participation of leading specialists from the scientific geophysical centers of Europe (Netherlands, Denmark, Poland, Austria, Finland, Hungary [Starostenko et al., 2009]. Along the PANCAKE profile, 14 sources were set up with an irregular step of 35—50 km (3 in Hungary and 11 in Ukraine). The reception was carried out by 261 autonomous digital TEXAN seismological stations, the step between which was also irregular and was, on average, about 2.5 km [Starostenko et al., 2013].

The high-quality seismic records made it possible to distinguish direct and refracted waves in the upper crust, the first arrivals of refracted waves in the lower crust, and reflected waves in the crust and from the Moho boundary. Refracted waves from the Moho boundary are also clearly visible on some records [Starostenko et al., 2009].

As a result, velocity models of the Earth's crust and upper mantle were constructed using ray modeling.

Finite-difference reflection/refraction migration is performed, taking into account the already-known velocity characteristics of the geological environment. Therefore, the obtained velocity model was taken before the application of migration. When processing the seismic wave fields observed along the PANCAKE profile, it was necessary to consider the area's complex tectonic structure. Finite-difference reflection/refraction migration was applied to a sample of tracks of each

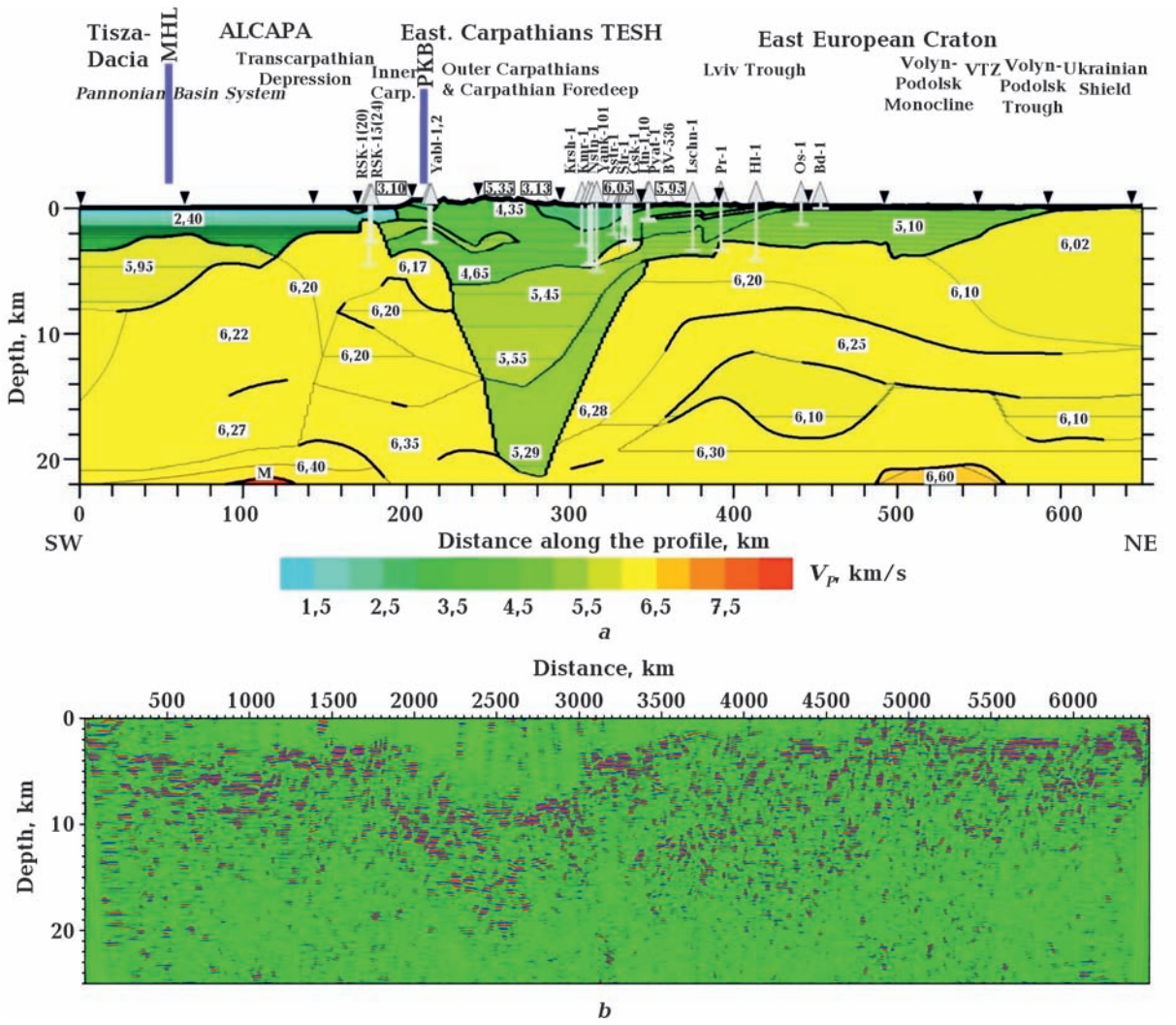

Fig. 4. The velocity model calculated using ray-tracing method (*a*) and the formed migration image of the upper crust (*b*) along the PANCAKE profile.

explosion point, and depth migration images were obtained up to a depth of 25 km.

For some shots in the center of the profile, two images were obtained from different sides of the source. To form a general image of the upper crust, all the migration results obtained for all 14 explosion points were analyzed, and all details and disturbances, depicted both from different sides of the source and at different removals, were considered.

Fig. 4 shows the velocity model calculated using ray modeling (Fig. 4, *a*) and the formed migration image of the upper crust (Fig. 4, *b*) along the PANCAKE profile. As can be seen from the figure, the combination of the result of kinematic processing (velocity model) and dynamic processing (migration image) allows to obtain more complete information about the structure of the research area.

The TTZ-South regional profile is about 550 km long. It runs along the southwestern edge of the East European Platform, partly in Poland and Ukraine [Janik et al., 2021]. Along the profile, 11 explosions were performed, recorded by 320 single-component stations (TEXAN and DATA-CUBE). The location of the TTZ-South profile on the map and the location of the explosions are shown in Fig. 3. Wave fields from 11 sources were processed using finite-difference reflection/refraction migration. For migration, in addition to the observed wave fields, the parameters of the velocity model of the environment calculated by the ray-tracing method were used as initial information [Janik et al., 2021]. Fig. 5 presents the results of ray-tracing (Fig. 5, *a*) and finite-difference reflection/refraction migration (Fig. 5, *b*) concerning the upper crust along the TTZ-South WARRP profile. The figure shows the coincidence of the results of kinematic and dynamic processing of the WARRP data in general terms. However, if these results are combined, the information that can be obtained from their joint interpretation will significantly increase.

Conclusions. Of course, the denser the observation system, the clearer and more detailed the geological environment image obtained with the help of seismic migration. Unfortunately, during regional seismic surveys, the location of sources and receivers is limited by various circumstances, so the irreg-

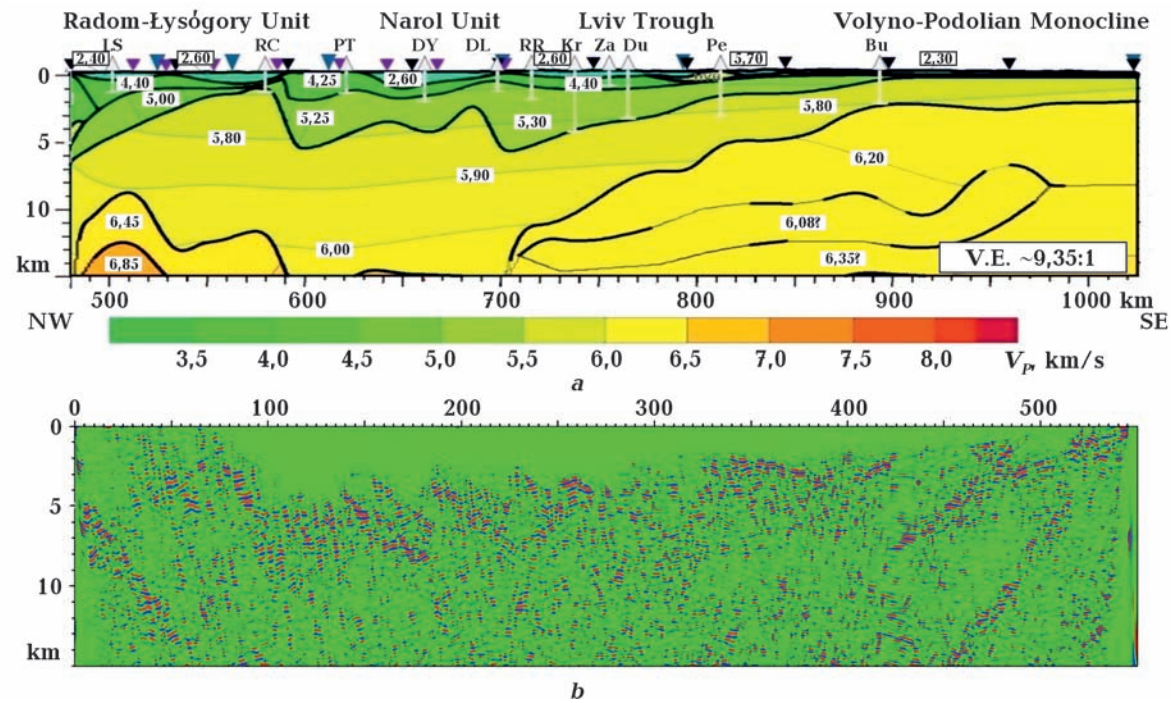

Fig. 5. The results of ray-tracing method (*a*) and finite-difference reflection/refraction migration (*b*) in relation to the upper crust along the TTZ-South WARRP profile.

ularity and sparseness of the observation system, and sometimes its insufficiency, require non-standard methods for processing the data registered in such conditions in order to obtain the most complete information about the deep structure of the area [Verpakhovskaya et al., 2021].

The practical examples confirmed that the finite-difference reflection/refraction migration method is currently the only possibility to reflect the geological structure in the dynamic characteristics of the wave field observed by the WARRP method.

The proofs of the correctness of the time and wave fields' continuations, which are performed by the finite-difference solution of differential equations — eikonal and the wave equation, allow us to discuss the accuracy of calculations when performing the finite-difference reflection/refraction migration.

The effectiveness of the application of the finite-difference reflection/refraction migration is demonstrated in the examples of wave fields observed along the regional profiles of the PANCAKE and TTZ-South. The application of the finite-difference reflection/refraction migration in the processing of PANCAKE and TTZ-South regional profile data showed that in areas with a complex depth structure, it is necessary to conduct a more thorough analysis of the migration images obtained for individual points of the explosion to reproduce their shape in the total migration section correctly.

The formed images of the upper crust along the PANCAKE and TTZ-South profiles made it possible to obtain additional information about the deep structure of the zone of transition from the Western European Platform to the Eastern European Platform. At the same time, combining the results of kinematic processing with ray-tracing method and dynamic processing with the finite-difference reflection/refraction migration allows to significantly increase the informativeness of the WARRP data.

References

Baysal, E., Kosloff, D.O., & Sherwood, J.W.C. (1983). Reverse time migration. *Geophysics, 48*, 1514—1524. https://doi.org/10.1190/1.1441434.

Claerbout, J.F. (1985). *Imaging the Earth's interior*. Oxford: Blackwell, 398 p.

Gardner, G.H.F. (Ed.). (1985). *Migration of Seismic Data*. Tulsa, OK, Society of Exploration Geophysicists Monograph Series, 462 p.

Godunov, S.K., & Ryabenkiy, V.S. (1977). *Difference schemes*. Moscow: Nauka, 440 p. (in Russian).

Janik, T., Starostenko, V., Aleksandrowski, P., Yegorova, T., Czuba, W., Środa, P., Murovskaya, A., Zajats, K., Kolomiyets, K., Lysynchuk, D., Wyjcik, D., Mechie, J., Głuszyński, A., Omelchenko, V., Legostaeva, O., Tolkunov, A., Amashukeli, T., Gryn, D., & Chulkov, S. (2021). TTZ-SOUTH seismic experiment. *Geofizicheskiy Zhurnal*, *43*(2), 28—44. https://doi.org/10.24028/gzh.v43i2.230189 (in Ukrainian).

Makris, J., Rihm, R., & Egloff, F. (1999). WARRP (Wide Aperture Reflection and Refraction Profiling): The principle of successful data acquisition where conventional seismic fails. *Seg Technical Program Expanded Abstracts*, 989—992. https://doi.org/18. 10.1190/1.1821279.

Murovskaya, A., Verpakhovska, O., Hnylko, O., Chorna, O., & Yegorova, T. (2023). Transcarpathian Depression: Study of Low-Velocity Zones in the Earth's Crust Based on the Seismic Regional Profiles Data. *Geofizicheskiy Zhurnal*, *45*(2). https://doi.org/10.24028/gj.v45i2.278310.

Pilipenko, V.N., Makris, J., Thibault, H., & Verpakhovskaya, A.O. (2003). Possible applications of the refraction migration in studies of the crustal structure. *Fizika Zemli,* (6), 94—101 (in Russian).

Pilipenko, V.N., & Verpakhovskaya, A.O. (2003). Features of migration transformation of the field of refracted waves. *Geofizicheskiy Zhurnal*, *25*(1), 42—55 (in Russian).

Pilipenko, V.M., Verpakhovska, O.O., Starostenko, V.I., & Pavlenkova, N.I. (2011). Wave images of the crustal structure from refractions andwide-angle reflections migration along the DOBRE profile (Dnieper-Donets paleorift). *Tectonophysics,* 508(1-4), 96—105. https://doi.org/10.1016/j.tecto.2010.11.009.

Samarskiy, A.A. (1983). *Theory of difference schemes*. Moscow: Nauka, 616 p. (in Russian).

Samarskiy, A.A., & Gulin, A.V. (1973). *Stability of difference schemes*. Moscow: Nauka, 416 p. (in Russian).

Samarskiy, A.A., & Popov, Yu.P. (1980). *Difference methods for solving gas dynamics problems*. Moscow: Nauka, 352 p. (in Russian).

Sinha, D.P., Vishnoi, D.K., Basu, S., & Singh, V.P. (2009). A brief comparison of the efficacy of four migration algorithms — a sub-basalt example. *Geohorizons*, 24—27.

Starostenko, V., Janik, T., Kolomiyets, K., Czuba, W., Sroda, P., Lysynchuk, D., Grad, M., Kovács, I., Stephenson, R., Lysynchuk, D., Thybo, H., Artemieva, I.M., Omelchenko, V., Gintov, O., Kutas, R., Gryn, D., Guterch, A., Hegedűs, E., Komminaho, K., Legostaeva, O., Tiira, T., & Tolkunov, A. (2013). Seismic velocity model of the crust and upper mantle along profile PANCAKE across the Carpathians between the Pannonian Basin and the East European Craton. *Tectonophysics, 608*, 1049—1072. https://doi.org/10.1016/j.tecto.2013.07.008.

Starostenko, V.I., Omelchenko, V.D., Lysynchuk, D.V., Legostaeva, O.V., Gryn, D.M., & Kolomiets, K.V. (2009). Study of the deep structure of the earth's crust and upper mantle along the Debrecen-Mukacheve-Rivne WARRP profile (PANCAKE-08 project). *Geoinformatics,* (2), 25—29 (in Ukrainian).

Sun, W., Fu, L.-Y., & Zhou, B. (2012).Common-angle image gathers for shot-profile migration: An efficient and stable strategy. *Exploration Geophysics, 43*(1), 1—7. https://doi.org/10.1071/EG11038.

Verpakhovskaya, O.O. (2021). Technique for the imaging crystalline basement according to the WARRP data. *Geofizicheskiy Zhurnal*, *43*(5), 127—149. https://doi.org/10.24028/gzh.v43i5.244076 (in Russian).

Verpakhovskaya, A., Pilipenko, V., & Budkevich, V. (2015). 3D finite-difference migration of the field of refracted waves. *Geofizicheskiy Zhurnal*, *37*(3), 50—65. https://doi.org/10.24028/gzh.0203-3100.v37i3.2015.111102 (in Russian).

Verpakhovska, A., Pilipenko, V., & Pylypenko, E. (2017). Formation geological depth image according to refraction and reflection marine seismic data. *Geofizicheskiy Zhurnal*, *39*(6), 106—121. https://doi.org/10.24028/gzh.0203-3100.v39i6.2017.116375 (in Russian).

Verpakhovskaya, O., Pylypenko, V., & Chornaya, O. (2021). Features of the seismic migration method in the RomUkrSeis profile data processing. *XXth Intern. Conf. on Geoinformatics: Theoretical and Applied Aspects, Kyiv, Ukraine, 10—13 May 2021* (pp. 1—6). https://doi.org/10.3997/2214-4609.20215521058.

Verpakhovskaya, A., Pylypenko, V., Yegorova, T., & Murovskaya, A. (2018). Seismic image of the crust on the PANCAKE profile across the UkrainianCarpathians from the migration method. *Journal of Geodynamics, 121*, 76—87. https://doi.org/10.1016/j.jog.2018.07.006.

White, R.S. (2020). Wide-angle refraction and reflection. *Regional Geology and Tectonics (Second Edition) Volume 1: Principles of Geologic Analysis*, 557—570. https://doi.org/10.1016/B978-0-444-64134-2.00019-5.

Yegorova, T., Verpakhovska, O., & Murovskaya, G. (2022). Three-layer structure of the Carpathian sedimentary prism from the results of seismic migration on the PANCAKE and RomUkrSeis WARR profiles. *Geofizicheskiy Zhurnal, 44*(2), 152—169. https://doi.org/10.24028/gj.v44i2.256270.

Zhang, Y., Xu, S., Tang, B., Bai, B., Huang, Y., & Huang, T. (2010). Angle gathers from reverse time migration *The Leading Edge*, 29, 1364—1371. http://dx.doi.org/10.1190/1.3517308.

Zhou, H.-W., Hu, H., Zou, Z., Wo, Y., & Youn, O. (2018). Reverse time migration: A prospect of seismic imaging methodology. *Earth-Science Reviews, 179*, 207—227. https://doi.org/10.1016/j.earscirev.2018.02.008.

Коректність скінченно-різницевих задач продовження часового та хвильового полів для міграційного зображення границі фундаменту

О. Верпаховська, О. Чорна, 2023

Інститут геофізики ім. С.І. Субботіна НАН України, Київ, Україна

У сучасній сейсморозвідці процедура міграції відіграє важливу роль для подальшої інтерпретації спостережених даних. Саме міграція дає можливість відобразити глибинну будову геологічного розрізу за динамічними характеристиками зареєстрованих хвильових полів.

При обробці даних глибинного сейсмічного зондування (ГСЗ, зарубіжний аналог WARRP (wide angle reflection/refraction profiling)), стандартні методи міграції є неефективними, що пов'язано з особливостями систем спостереження. Всі існуючі методи міграції переважно ґрунтуються на відбитих хвилях, які мають обмежений інтервал реєстрації. Хвильове поле при ГСЗ спостерігається на відстанях від джерел, які сягають кількох сотень кілометрів, нерегулярний крок між приймачами становить в середньому 1—3 км. За таких умов складно, а іноді й неможливо виділити відбиті хвилі.

Розроблена в Інституті геофізики ім. С.І. Субботіна НАН України модель скінченно-різницевої міграції поля відбитих/рефрагованих хвиль довела свою ефективність при побудові міграційних зображень глибинної будови розрізу за даними ГСЗ, спостереженими в різних регіонах світу. Основною відмінністю даного методу міграції є використання рефрагованих хвиль як опорних, зареєстрованих у віддаленій зоні джерела. Водночас виникає питання коректності відтворення глибинної будови розрізу на міграційному зображенні, що залежить від коректності методів розрахунку. Алгоритм скінченно-різницевої міграції поля відбитих/рефрагованих хвиль містить продовження часового та хвильового полів. Наведено доказ математичної коректності розв'язання диференціальних рівнянь ейконалу та скалярного хвильового рівняння скінченно-різницевим методом, на яких ґрунтуються продовження часового та хвильового полів відповідно.

Зіставлення сформованих міграційних зображень та швидкісних моделей, розрахованих променевим моделюванням верхньої кори вздовж профілів PANCAKE та TTZ-South, дає можливість стверджувати, що поєднання результатів кінематичної та динамічної обробки даних ГСЗ підвищує інформативність їх подальшої інтерпретації.

Ключові слова: коректність, міграція відбитих/заломлених хвиль, зворотне продовження хвильового поля, пряме продовження часового поля, профілі DSS (WARRP), рівняння ейконалу, хвильове рівняння.